

## Extensive load in multitasking associative networks

Peter Sollich,<sup>1</sup> Daniele Tantari,<sup>2</sup> Alessia Annibale,<sup>3,4</sup> and Adriano Barra<sup>5</sup>

<sup>1</sup>*Department of Mathematics, King's College London, Strand, London WC2R 2LS, U.K.*

<sup>2</sup>*Dipartimento di Matematica, Sapienza Università di Roma, P.le Aldo Moro 2, 00185, Roma, Italy.*

<sup>3</sup>*Institute for Mathematical and Molecular Biomedicine,*

*King's College London, Hodking Building, London SE1 1UL, U.K.*

<sup>4</sup>*Mathematics Department, King's College London, The Strand WC2R 2LS, London, UK.*

<sup>5</sup>*Dipartimento di Fisica, Sapienza Università di Roma, P.le A. Moro 2, 00185, Roma, Italy.*

(Dated: February 29, 2024)

We use belief-propagation techniques to study the equilibrium behavior of a bipartite spin-glass, with interactions between two sets of  $N$  and  $P = \alpha N$  spins. Each spin has a finite degree, i.e. number of interaction partners in the opposite set; an equivalent view is then of a system of  $N$  neurons storing  $P$  diluted patterns. We show that in a large part of the parameter space of noise, dilution and storage load, delimited by a critical surface, the network behaves as an extensive parallel processor, retrieving all  $P$  patterns *in parallel* without falling into spurious states due to pattern cross-talk and typical of the structural glassiness built into the network. Our approach allows us to consider effects beyond those studied in replica theory so far, including pattern asymmetry and heterogeneous dilution. Parallel extensive retrieval is more robust for homogeneous degree distributions, and is not disrupted by biases in the distributions of the spin-glass links.

PACS numbers: 07.05.Mh, 87.19.L-, 05.20.-y

Since their introduction in the pioneering paper by Amit Gutfreund and Sompolinsky [1, 2], associative neural networks (NN) have played a central role in the statistical mechanics community, soon becoming one of the most successful offshoots of spin glasses (SG) [3], as proved by the celebrated paper by Hopfield [4] or the excellent book by Amit [5].

Indeed, the Hopfield model for NN [4] can be regarded as a SG where the coupling between each pair of spins  $\sigma_i, \sigma_j$ ,  $i, j = 1, \dots, N$  has the Hebbian form  $J_{ij} = N^{-1} \sum_{\mu} \xi_i^{\mu} \xi_j^{\mu}$  and the  $\xi^{\mu}$ ,  $\mu = 1, \dots, P = \alpha N$ , represent stored patterns with entries  $\xi_i^{\mu} = \pm 1$  distributed as  $P(\xi_i^{\mu} = \pm 1) = 1/2$ . Replica analysis shows that, in the thermodynamic limit, this system exhibits an ordered structure of the free energy minima in the low noise regime and for storage load  $\alpha < \alpha_c \sim 0.14$  (within the “replica symmetric” ansatz). For higher loads the NN becomes equivalent to the Sherrington-Kirkpatrick SG [3], as  $\sqrt{N}J_{ij}$  becomes Gaussian with unit variance by a simple central limit theorem argument [6, 7].

A further connection between NN and SG has been pointed out recently in the context of bipartite SG [8]. Consider a system of two sets of spins,  $\sigma_i$ ,  $i = 1, \dots, N$  and  $\tau_{\mu}$ ,  $\mu = 1, \dots, P$ , connected by links  $\xi_i^{\mu} = \pm 1$  that are now *sparse* so that  $P(\xi_i^{\mu} = \pm 1) = c/2N$  and  $P(\xi_i^{\mu} = 0) = 1 - c/N$  with  $c = \mathcal{O}(N^0)$ , and described by the SG Hamiltonian  $H_{SG}(\sigma, \tau | \xi) \propto - \sum_{i, \mu} \xi_i^{\mu} \sigma_i \tau_{\mu}$ . Marginalizing over  $\tau$  in the partition function  $Z = \sum_{\sigma, \tau} e^{-\beta H_{SG}(\sigma, \tau | \xi)} = \sum_{\sigma} e^{-\beta H_{NN}(\sigma | \xi)}$  shows that the  $\sigma$  represent a NN with Hamiltonian  $H_{NN}(\sigma | \xi) = -\beta^{-1} \sum_{\mu} \ln[2 \cosh(\beta \sum_i \xi_i^{\mu} \sigma_i)]$  or, up to an additive constant,  $H_{NN}(\sigma | \xi) = -\frac{\beta}{2} \sum_{\mu, i, j} (\xi_i^{\mu} \xi_j^{\mu}) \sigma_i \sigma_j + \dots$ . Higher order interactions are not written explicitly here; these are fully absent if the  $\tau_i$  are continuous rather than discrete and have a Gaussian prior.

At variance with standard NN models, the pattern entries in  $H_{NN}(\sigma | \xi)$  are diluted since the corresponding bipartite SG is sparse. While standard NN retrieve patterns sequentially (one at time), associative networks with diluted patterns, as resulting from the marginalization of a diluted bipartite SG, are able to accomplish parallel retrieval in appropriate dilution regimes [9, 10, 12, 13]. We note that, in contrast, diluting NNs by removing links among neurons only results in a weakening of the sequential retrieval [5]. Beyond their applications in biology [10] and potentially large impact in artificial intelligence for their parallel processing capabilities, associative networks with diluted patterns reveal the inextricable link between the (sparse) bipartite network topology and the (parallel) mode of associative network operation. So far, diluted associative networks have been studied via replica analysis [10], for pattern-independent dilution. This setting only accounts for special structures of the underlying bipartite graph, with all degrees in each set drawn from the same Poisson distribution. Here we use cavity (i.e. belief-propagation) methods to analyze the more general scenario where degrees in the two sets of spins have arbitrary distributions, thus allowing for a much greater variety of bipartite network structures.

We consider an equilibrated system of  $N$  binary neurons  $\sigma_i = \pm 1$  at temperature (fast noise)  $T = 1/\beta$ , with Hamiltonian

$$H(\sigma | \xi) = -\frac{1}{2} \sum_{i, j} \sum_{\mu} \xi_i^{\mu} \xi_j^{\mu} \sigma_i \sigma_j,$$

where pattern entries  $\{\xi_i^{\mu}\}$  are sparse (i.e. the number of non-zero entries of a pattern is finite) [17]. We can then use a factor graph representation of the Boltzmann

weight as  $\prod_{\mu} F_{\mu}$ , with factors

$$F_{\mu} = e^{(\beta/2) \sum_{i,j \in O(\mu)} \xi_i^{\mu} \xi_j^{\mu} \sigma_i \sigma_j} = \langle e^{z \sum_{i \in O(\mu)} \xi_i^{\mu} \sigma_i} \rangle_z, \quad (1)$$

where  $O(\mu) = \{i : \xi_i^{\mu} \neq 0\}$  and  $z$  is a zero mean Gaussian variable with variance  $\beta$  [18]. We denote by  $e_{\mu} = |O(\mu)|$  the degree of a pattern  $\mu$  and by  $d_i = |N(i)|$  the degree of a neuron  $i$ , with  $N(i) = \{\mu : \xi_i^{\mu} \neq 0\}$ . We consider random graph ensembles with given degree distributions  $P(d)$  and  $P(e)$ , and nonzero  $\xi$ 's independently and identically distributed (i.i.d.). Conservation of links demands  $N\langle d \rangle = P\langle e \rangle$  where averages are taken over  $P(d)$  and  $P(e)$ . The *message* from factor  $\mu$  to node  $i$  is the cavity distribution  $P_{\mu}(\sigma_j)$  of  $\sigma_j$  when this is coupled to factor  $\mu$  only, which we can parametrize by an effective field  $\psi_{\mu \rightarrow j}$ . The message from node  $j$  to factor  $\mu$  is the cavity distribution  $P_{\setminus \mu}(\sigma_j)$  of  $\sigma_j$  when coupled to all factors except  $\mu$ , which we can parametrize by the field  $\phi_{j \rightarrow \mu}$ . The cavity equations are then [11]

$$P_{\mu}(\sigma_j) = \text{Tr}_{\{\sigma_k\}} F_{\mu}(\sigma_j, \{\sigma_k\}) \prod_{k \in O(\mu) \setminus j} P_{\setminus \mu}(\sigma_k), \quad (2)$$

$$P_{\setminus \nu}(\sigma_j) = \prod_{\mu \in N(j) \setminus \nu} P_{\mu}(\sigma_j), \quad (3)$$

and translate to equations for the effective fields:

$$\psi_{\mu \rightarrow j} = \tanh^{-1} \langle \sigma_j \rangle_{\mu} = \quad (4)$$

$$\tanh^{-1} \frac{\langle \sinh(z \xi_j^{\mu}) \prod_{k \in M(\mu) \setminus j} \cosh(\phi_{k \rightarrow \mu} + z \xi_k^{\mu}) \rangle_z}{\langle \cosh(z \xi_j^{\mu}) \prod_{k \in M(\mu) \setminus j} \cosh(\phi_{k \rightarrow \mu} + z \xi_k^{\mu}) \rangle_z},$$

$$\phi_{j \rightarrow \nu} = \sum_{\mu \in N(j) \setminus \nu} \psi_{\mu \rightarrow j}. \quad (5)$$

These equations, once iterated to convergence, are exact on tree graphs. They will also become exact on graphs sampled from our ensemble in the thermodynamic limit of large  $N$ , because the sparsity of the  $\xi_i^{\mu}$  makes the graphs locally tree-like, with typical loop lengths that diverge (logarithmically) with  $N$ .

For large  $N$ , we can describe the solution of the cavity equations on any fixed graph – and hence also the quenched average over the graph ensemble and the nonzero pattern entries  $\xi_i^{\mu}$  – in terms of the distribution of messages or fields,  $W_{\psi}(\psi)$  and  $W_{\phi}(\phi)$ . Denoting by  $\Psi(\{\phi_{k \rightarrow \mu}\}, \{\xi_k^{\mu}\}, \xi_j^{\mu})$  the r.h.s. of (4), convergence of the cavity iterations then implies the self-consistency equation

$$W_{\psi}(\psi) = \sum_e \frac{eP(e)}{\langle e \rangle} \langle \delta(\psi - \Psi(\phi_1, \dots, \phi_{e-1}, \xi^1, \dots, \xi^e)) \rangle$$

where the average is over i.i.d. values of the (nonzero)  $\xi^1, \dots, \xi^d$  and over i.i.d.  $\phi_1, \dots, \phi_{e-1}$  drawn from  $W_{\phi}(\phi)$ , and similarly

$$W_{\phi}(\phi) = \sum_d \frac{dP(d)}{\langle d \rangle} \langle \delta\left(\phi - \sum_{\mu=1}^{d-1} \psi_{\mu}\right) \rangle,$$

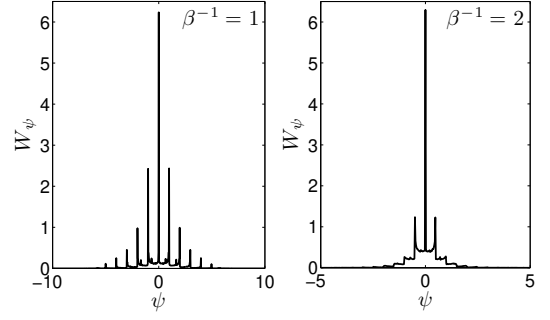


FIG. 1: Histograms  $W_{\psi}(\psi)$  of the field  $\psi$  for  $\alpha = 8$ ,  $c = 2$  and  $\beta^{-1} = 1, 2$ , as shown in figure.

where the average is over i.i.d.  $\psi_1, \dots, \psi_{d-1}$  drawn from  $W_{\psi}(\psi)$ . Field distributions can then be obtained numerically by population dynamics (PD) [15]. For symmetric  $\xi$ -distributions, a delta function at the origin for both  $W_{\psi}$ ,  $W_{\phi}$  is always a solution, and we find this to be stable at high temperatures. At low  $T$ , the  $\psi$  can become large (see Fig. 1), hence also the  $\phi$ , and spins  $\sigma_i$  will typically be strongly polarized. The fields  $\beta \xi_i^{\mu} \sum_{j \in O(\mu) \setminus i} \xi_j^{\mu} \sigma_j$  then fluctuate little, and the  $\psi$  as suitable averages of these fields cluster near multiples of  $\beta$  (for  $\xi = \pm 1$ ).

Our main interest is in the retrieval properties, encoded in the fluctuating pattern overlaps  $m_{\mu} = \sum_{i \in M(\mu)} \xi_i^{\mu} \sigma_i$ . Since the joint distribution of the  $\sigma_i$  in  $M(\mu)$  is  $F_{\mu}(\{\sigma_i\}) \prod_{i \in M(\mu)} P_{\setminus \mu}(\sigma_i)$ , the distribution of the pattern overlap is

$$\frac{\text{Tr}_{\{\sigma_i\}} \langle \delta(m_{\mu} - m) \exp(\sum_{i \in M(\mu)} (\xi_i^{\mu} z + \phi_{i \rightarrow \mu}) \sigma_i) \rangle_z}{\text{Tr}_{\{\sigma_i\}} \langle \exp(\sum_{i \in M(\mu)} (\xi_i^{\mu} z + \phi_{i \rightarrow \mu}) \sigma_i) \rangle_z}. \quad (6)$$

Defining this as  $\mathcal{P}(m, \{\phi_{i \rightarrow \mu}\}, \{\xi_i^{\mu}\})$ , in the graph ensemble we have

$$P(m) = \sum_e P(e) \langle \mathcal{P}(m, \phi_1, \dots, \phi_e, \xi_1, \dots, \xi_e) \rangle. \quad (7)$$

The average here can be read as  $P(m|e)$ , the overlap distribution for patterns with fixed degree  $e$ . Whenever  $W_{\phi}(\phi) = \delta(\phi)$ ,  $P(m|e)$  is the overlap distribution for an “effectively isolated” subsystem of size  $e$ : the neurons storing each pattern  $\xi^{\mu}$  can retrieve this independently of other patterns, even though the number of patterns is extensive. Retrieval within each group of neurons is strongest at low temperatures (see Fig. 2 left) as expected on general grounds. Once nonzero  $\phi$  appear neuron groups are no longer independent: intuitively, cross-talk interference between patterns emerges.

*Bifurcation* – When the “parallel processor” solution with zero cavity fields  $\phi$  becomes unstable, a bifurcation to a different stable solutions occurs. Depending on the external parameters, this can be seen in the first or second moment of the field distribution. Expanding for

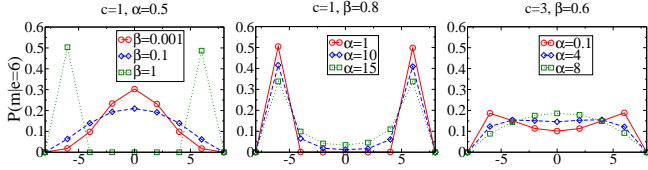


FIG. 2:  $P(m|e=6)$  above (left) and crossing (middle and right) the critical line for different values of  $\beta$  and  $\alpha$ , respectively. Full red (dashed blue and dotted green) curves in the middle and right panels refer to temperatures above (below) the critical line.

small fields we get

$$\Psi(\{\phi_{k \rightarrow \mu}\}, \{\xi_k^\mu\}, \xi_j^\mu) \approx \sum_{k \in O(\mu) \setminus j} \phi_{k \rightarrow \mu} \Xi(\xi_k^\mu, \xi_j^\mu, \{\xi_l^\mu\})$$

with coefficients  $\Xi(\xi_k^\mu, \xi_j^\mu, \{\xi_l^\mu\})$  given by

$$\frac{\langle \sinh(z\xi_j^\mu) \sinh(z\xi_k^\mu) \prod_{l \in O(\mu) \setminus \{j,k\}} \cosh(z\xi_l^\mu) \rangle_z}{\langle \prod_{l \in O(\mu)} \cosh(z\xi_l^\mu) \rangle_z}.$$

The self-consistency relations for the field distributions  $W_\psi$  and  $W_\phi$  then show that as long as the mean fields are small, they are related to leading order by

$$\langle \psi \rangle = \langle \phi \rangle \sum_e P(e) \frac{e(e-1)}{\langle e \rangle} \langle \Xi(\xi_1, \dots, \xi_e) \rangle \quad (8)$$

$$\langle \phi \rangle = B_d \langle \psi \rangle \quad (9)$$

where  $B_d = \sum_d P(d) d(d-1) / \langle d \rangle$  is one of the two branching ratios of our locally tree-like graphs, the other being  $B_e = \sum_e P(e) e(e-1) / \langle e \rangle$ . If the means are zero then the onset of nonzero fields is detected by the variances, which are related to leading order by

$$\langle \psi^2 \rangle = \langle \phi^2 \rangle \sum_e P(e) \frac{e(e-1)}{\langle e \rangle} \langle \Xi^2(\xi_1, \dots, \xi_e) \rangle \quad (10)$$

$$\langle \phi^2 \rangle = B_d \langle \psi^2 \rangle \quad (11)$$

*Symmetric pattern distributions* – When the  $\xi$  are symmetrically distributed, then also the field distributions are always symmetric and there can be no instability from growing means; cf. (8). The bifurcation has to result from the growth of the variances, which from (11) occurs at  $A = 1$  with

$$A = B_d \sum_e P(e) \frac{e(e-1)}{\langle e \rangle} \langle \Xi^2(\xi_1, \dots, \xi_e) \rangle \quad (12)$$

This factorizes as  $A = B_d A_e(\beta)$  with the dependence on the noise and the distribution of the  $e$ 's contained in the second factor  $A_e(\beta)$ . For  $\beta \rightarrow 0$  the variance of  $z$  goes to zero and  $A_e(0) = 0$ . For  $\beta \rightarrow \infty$ , the  $z$ -averages are dominated by large values of  $z$  where  $\sinh^2(z) \approx \cosh^2(z)$ , so  $A_e(\infty) = B_e$ . Hence there is no bifurcation when  $B_d B_e < 1$ , in agreement with the

general bipartite tree percolation condition [16]. For the case  $P(\xi_i^\mu = \pm 1) = c/(2N)$  considered in [10], the distributions of pattern degrees  $e$  and neuron degrees  $d$  are Poisson( $c$ ) and Poisson( $\alpha c$ ), respectively, so  $B_d = \alpha c$ ,  $B_e = c$  and there is no bifurcation for  $\alpha c^2 < 1$ . The network acts as a parallel processor here for *any*  $T$  because the bipartite network consists of finite clusters of interacting spins in which there is no interference between different patterns [10]. At higher connectivity, the critical line defined by  $A = 1$  indicates the temperature above which this lack of interference persists even though the network now has a giant connected component. Fig. 3 (left) compares theory to PD results, where we locate the transition as the onset of nonzero second moments of the field distributions. The impact of the transition on the overlap probability distribution of a pattern with fixed  $e$  can be seen from the PD results in Fig. 2 (middle and right panels). Crossing the transition line, parallel retrieval is accomplished at low temperatures, but it degrades when  $\alpha$  is increased (see shrinking peaks in the middle panel), or  $c$  is increased, eventually fading away for sufficiently large  $\alpha$  and  $c$  (right panel).

One advantage of our present method is that we can easily investigate the parallel processing capabilities of a bipartite graph with arbitrary degrees  $\{e_\mu\}$ . Here we have a pattern-dependent dilution of the links  $P(\xi) \propto \prod_{i,\mu} P(\xi_i^\mu) \prod_{\mu} \delta_{e_\mu, \sum_i |\xi_i^\mu|}$  with

$$P(\xi_i^\mu) = \frac{e_\mu}{2N} (\delta_{\xi_i^\mu, 1} + \delta_{\xi_i^\mu, -1}) + (1 - \frac{e_\mu}{N}) \delta_{\xi_i^\mu, 0} \quad (13)$$

leading to  $P(d) = \text{Poisson}(\alpha \langle e \rangle)$  while  $P(e) = P^{-1} \sum_{\mu} \delta_{e, e_\mu}$ . If we keep the mean degree fixed  $\langle e \rangle = c$ , the critical point for  $\beta \rightarrow \infty$  is found at

$$B_d B_e = \alpha c (\langle e^2 \rangle / c - 1) = \alpha [c(c-1) + \text{Var}(e)] = 1$$

while for large  $\alpha$  one obtains for the critical line  $\beta_c^{-1}(\alpha) \approx \sqrt{\alpha} \sqrt{c(c-1) + \text{Var}(e)}$ . Similar results are obtained with soft constraints  $e_\mu$  on the degrees, i.e. by dropping the delta function constraint in  $P(\xi)$  before (13): one now finds  $B_d B_e = \alpha(c^2 + \text{Var}(e))$  and  $\beta_c^{-1}(\alpha) \approx \sqrt{\alpha} \sqrt{c^2 + \text{Var}(e)}$ . In both cases, the region where parallel retrieval is obtained is larger for degree distributions with smaller variance; the optimal situation occurs when all patterns have exactly the same number  $c$  of non zero entries (Fig. 3, right).

*Non-symmetric pattern distributions* – To introduce a degree of asymmetry  $a \in [-1, +1]$  in the pattern distribution, we next take for the nonzero pattern entries  $P(\xi_i^\mu = \pm 1) = (1 \pm a)/2$ . Evaluating the  $\xi$ -average  $\langle \Xi(\dots) \rangle$  in (8), the condition for a transition to nonzero field means then becomes

$$1 = a^2 B_d \sum_e P(e) \frac{e(e-1)}{\langle e \rangle} \frac{\langle \sinh^2(z) \cosh^{e-2}(z) \rangle_z}{\langle \cosh^e(z) \rangle_z} \quad (14)$$

At zero temperature the bifurcation occurs when  $B_d B_e = a^{-2}$ ; when  $a$  tends to zero the transition point goes to

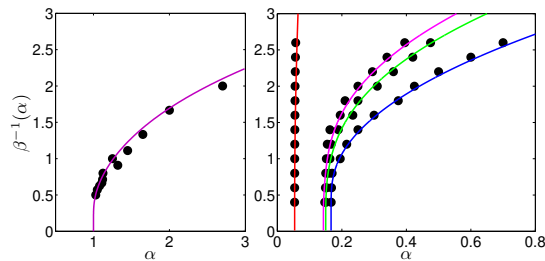


FIG. 3: Transition lines (theory, with symbols from PD numerics) for different pattern degree distributions. Left:  $e \sim \text{Poisson}(c=1)$ . Right: changing  $P(e)$  at constant  $\langle e \rangle = 3$ ;  $P(e) = \delta_{e,3}$  (blue);  $P(e) = (\delta_{e,2} + \delta_{e,3} + \delta_{e,4})/3$  (green);  $P(e) = (\delta_{e,2} + \delta_{e,4})/2$  (pink);  $P(e)$  power law as in preferential attachment graphs, with  $\langle e^2 \rangle = 21.66$  (orange).

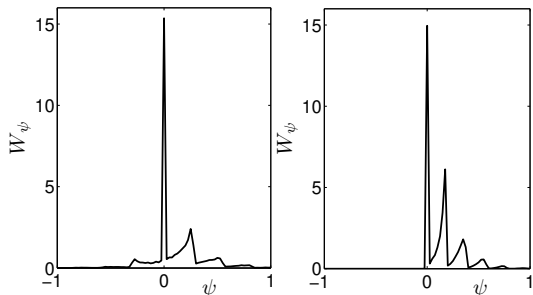


FIG. 4: Histogram of the fields  $\psi$  in the ferromagnetic region, for  $c = 1$ ,  $\beta = 1$  and different levels of bias:  $a = 0.9$  with  $\alpha = 9$  (left) and  $a = 1$  with  $\alpha = 8$  (right). Field distributions are obtained by PD starting from positive fields, to break the gauge symmetry. For  $a = 1$  (right) there are only positive fields as expected: when all patterns have positive entries there are no conflicting signals, even above the percolation threshold.

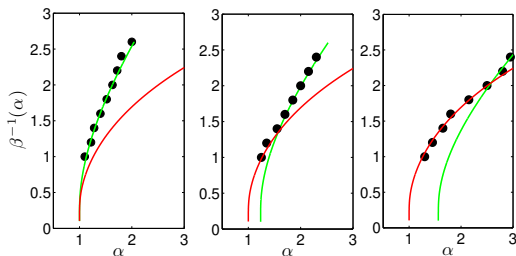


FIG. 5: Transition lines to growing field means (theory, green) and variances (theory, red), showing a good match to numerical PD data (dots); here  $c = 1$  and pattern bias  $a = 1, 0.95, 0.9$  from left to right. The first line to be crossed from high  $T = \beta^{-1}$  gives the physical transition.

infinity and we retrieve the symmetric case. Beyond the bifurcation, non-centered field probability distribu-

tions (see Fig. 4) produce a non-zero global magnetization typical of ferromagnetic systems. One has to bear in mind, however, that even with a bias in the pattern entry distribution a bifurcation to growing field variances at zero means can occur; the physical bifurcation is the one occurring first on lowering  $T$ . Numerical evaluation shows that both bifurcation temperatures increase with  $\alpha$ . For large  $\alpha$  one can then resort to a low- $\beta$  expansion:  $\langle \sinh^2(z) \cosh^{e-2}(z) \rangle \approx \langle z^2 \rangle = \beta$ ,  $\langle \cosh^e(z) \rangle \approx 1$ . This gives for the growing mean bifurcation condition  $1 \approx B_d B_e \beta a^2$  while for the growing variance bifurcation  $1 \approx B_d B_e \beta^2$ . For Poisson graphs  $B_d B_e = \alpha c^2$ , giving the transition lines  $\beta_{c,1}^{-1}(\alpha) \approx c^2 a^2 \alpha$  and  $\beta_{c,2}^{-1}(\alpha) \approx c \sqrt{\alpha}$  for large  $\alpha$ . In the presence of a nonzero pattern bias  $a$  these cross at  $\alpha = 1/(ca^2)$ , with the bifurcation to growing means occurring first for larger  $\alpha$ . The existence of this crossing is confirmed by numerical evaluation of (12) and (14) for finite  $\alpha$  in Fig. 5.

In conclusion, we have developed a cavity/belief-propagation framework to analyse finitely connected bipartite spin glasses, with arbitrary structure and an arbitrary degree of asymmetry in the link distribution, as well as thermodynamically equivalent associative networks with diluted patterns. Extensive multitasking features appear quite naturally in these systems. Our framework has enabled us to investigate their robustness for arbitrary pattern degree distributions and asymmetry, by locating the transition surface that separates the region in  $(\alpha, \beta, c)$ -space where the network is capable of parallel extensive retrieval, from the region where pattern interference affects the network performance as a parallel processor. Our results show that homogeneous degree distributions in the bipartite network favour parallel retrieval. In addition, we find that a biased distribution of the sparse pattern entries can yield a macroscopic net magnetization and shrinks the region of parameter space where no pattern cross-talk occurs. However, we note that in the ferromagnetic region, pattern cross-talk may result in a constructive interference between patterns, which does not disrupt the parallel retrieval performed by the network. Our analysis makes contact with previous replica calculations [10, 12] for homogeneous graphs with symmetrically distributed links. In addition, the cavity framework allows for straightforward extensions to general graph topology and link distributions, and may lead to a broad range of applications, from biological to artificial systems.

AB and DT acknowledge the FIRB grant RBF08EKEV, Sapienza University and GNFM-INdAM for financial support. PS acknowledges funding from the EU under REA grant agreement nr. 290038 (NETADIS). Elena Agliari is acknowledged for helpful interactions.

[1] D. J. Amit, H. Gutfreund, H. Sompolinsky, *Phys. Rev. Lett.* **55**, 1530, (1985).

[2] D.J. Amit, H. Gutfreund, H. Sompolinsky, *Ann. of Phys.*

- 173**(1):30-67, (1987).
- [3] M. Mezard, G. Parisi, M.A. Virasoro, *Spin glass theory and beyond*, 9. Singapore: World scientific, (1987).
- [4] J.J. Hopfield, *Proc. Natl. Acad. Sci. USA* **79**(8):2554-2558, (1982).
- [5] D.J. Amit, *Modeling brain function*, Cambridge University Press, (1992).
- [6] A. Barra, F. Guerra, *J. Math. Phys.* **49**:125217, (2008).
- [7] A.C.C. Coolen, R. Kühn, P. Sollich, *Theory of Neural Information Processing Systems*, Oxford Press, Oxford, (2005).
- [8] E. Agliari, et al., *J. Theor. Biol.* **287**:48-63, (2011).
- [9] E. Agliari, et al., *Phys. Rev. Lett.* **142**, 2313, (2012).
- [10] E. Agliari, et al., *J. Phys. A* **46**, 415003, (2013).
- [11] M. Mezard and G. Parisi, *Eur. Phys. J. B* **20**, 217 (2001).
- [12] E. Agliari, et al., *J. Phys. A* **46**, 335101, (2013).
- [13] D.E. Rumelhart, J. L. McClelland, G. E. Hinton, *Parallel distributed processing: Explorations in the microstructure of cognition*, (1986).
- [14] M.J. Urry, P. Sollich, *J. Mach. Learn. Res.* **14**, 1801:1835, (2013).
- [15] M. Mezard, G. Parisi, *Eur. Phys. J. B* **20**, 217, (2001).
- [16] M. E. J. Newman, et al., *Phys. Rev. E*, **64**(2):026118(2001)
- [17] We omit the factor  $\beta$  from  $H_{NN}(\sigma|\xi)$  so that our  $\beta$  corresponds to  $\beta^2$  in the bipartite SG.
- [18] Eq. (1) corresponds to Gaussian  $\tau_i$  in the bipartite SG, at our redefined  $\beta$ ; for discrete  $\tau_i$  one would average over  $z = \pm\beta$  with probability 1/2 each.